Exploring Thin Glass Strength Test Methodologies

Oliveira Santos, Francisco; Louter, Christian; Ramôa Correia, João

Important note
To cite this publication, please use the final published version (if applicable).
Please check the document version above.

Exploring Thin Glass Strength Test Methodologies

Francisco Oliveira Santos [a, b], Christian Louter [b], João Ramôa Correia [c]

[a] Instituto Superior Técnico, University of Lisbon, Portugal, francisco.osantos@gmail.com
[b] Delft University of Technology, The Netherlands
[c] CERIS, Instituto Superior Técnico, University of Lisbon, Portugal

Thin glass is currently widespread in mobile devices and has great potential for applications in buildings. However, presently there is no standard method to determine the strength of thin glass for building applications and there is little experimental data available on its mechanical behaviour. Hence, this paper presents experimental and numerical investigations developed with two main goals: (i) to assess and (eventually) adapt existing test setups in order to determine the strength of thin glass; and (ii) to characterize thin glass using those tests, focusing on the ultimate strength of the material. The experimental programme, which was executed at TU Delft, comprised destructive tests on chemically tempered thin glass (thickness of 2 mm). Two destructive tests were assessed and tentatively improved: the in-plane four-point bending test, which involved many difficulties related with geometrical and mechanical instabilities; and the buckling test, which provided a lower bound for the material strength, as failure was triggered in the supports (due to stress concentrations). Based on the results obtained, a new tension test was proposed and numerically investigated; the results obtained revealed many advantages over the former tests in terms of quality/consistency of results and possibility of standardization.

Keywords: thin glass; strength; material characterization; destructive testing; numerical modelling.

1. Introduction

Thin glass usually refers to glasses with thickness below 2 mm (Albus & Robanus, 2015), particularly in the range of 0.55 mm to 2.00 mm (Neugebauer, 2015). In terms of composition, thin glass can for instance be made of soda-lime glass or aluminosilicate glass. Usually, these glasses are produced using either the float, micro-float (Schneider, 2015), the down-draw (SCHOTT, 2014 a) or the overflow-fusion (Corning, 2016) processes. Subsequent tempering of aluminosilicate glass is typically done by means of chemical tempering, whereas soda-lime silicate glass can be either chemically or thermally tempered (Neugebauer, 2016b) Thin glass presents a combination of high strength and small thicknesses that results in a flexible material with a wide range of applications. In the current paper, thin glass refers to aluminosilicate chemically tempered glass.

There is a broad range of industries where thin glass has potential to be applied. In buildings, thin glass could be used: (i) as flat panels, such as in tensile façades or overhead glazing with long spans, where its high strength provides significant advantages and its low self-weight would be a benefit; (ii) as cold-bent panels, such as in any curved design or membrane structures replacing the expensive process of bending glass; or (iii) in adaptive or dynamic designs, making use of its flexibility in applications such as moveable elements, e.g., stadium roofs or canopies, or adaptive façades. All those structural applications require determining the tensile strength of thin glass.

Considering the standard methods to test the strength of glass, namely the EN ISO 1288, it is clear that the geometrical nonlinearities thwart the correct procedure and calculations of the strength of thin glass. In fact, the relevant tests comprised by this norm are two coaxial double ring tests and a four-point bending test; while the first is used for applications where the edge is not loaded, the latter also stresses the edge. It is worth mentioning that both tests assume small deformations and the Bernoulli theory, so the deformations are limited up to a percentage of the thickness.

A few recent studies focused on testing the strength of thin glass, namely those of Siebert (2013), Spitzhüttl *et al.* (2014), Maniatis *et al.* (2014) and Neugebauer (2016a). In a first phase, these studies focused on the standard tests of EN ISO 1288, and then proposed alternative testing protocols. The next paragraphs summarize their main findings about both the standard tests (double coaxial tests and four-point bending tests) and the alternative protocols, including the multiple point bending test and the buckling test.

In European standard, two coaxial double ring tests are specified: the EN ISO 1288-2, with rings of larger diameters for larger applications, and the EN ISO 1288-5, with smaller rings for smaller applications. Even for smaller samples, Neugebauer (2016a) confirms the need to take into account geometrical nonlinearities (key factor), size effects and imperfections of the setup or glass plate. His experimental and numerical tests revealed large asymmetric deformations. Stresses were not uniform on the stressed area.

For the four-point bending test, described in EN ISO 1288-3, the deformations are simply too large when testing thin glass. Maniatis *et al.* (2014) proposed using the same dimensions for the setup, but with a modified analytical approach to include the geometrical nonlinearities, such as the horizontal reaction forces developed at the supports. In this study, experiments were also conducted in fully tempered thin glass samples. However, this setup becomes impracticable for higher strength values or lower thicknesses: considering a 2 mm thick chemically tempered glass plate with strength of 600 MPa to 800 MPa, the ultimate curvature radius

would be between 90 mm and 120 mm; for smaller thicknesses, it would be even lower. The plate would simply slip between the supports before being fractured.

A modification to this setup was proposed by Siebert (2013) and Neugebauer (2016), the multiple-point bending test, which consists of several pairs of loads and supports in order to introduce maximum stresses on a considerable length, but distributed over several smaller loading spans. One of the main drivers for this setup is the possibility to use the standard 1100×360 mm^2 plates. Nonetheless, according to the authors' knowledge, the setup has not yet been validated experimentally; moreover, it presents many difficulties, such as its sensitivity to imperfections in the setup geometry.

Finally, another test presented in all of the above-mentioned studies is the buckling test. In this case, the glass panel is vertically supported by two rollers that rotate about the weak axis of inertia of the plate and is loaded by an in-plane force at the top; the force triggers the buckling of the plate and an increasing out-of-plane deflection. Spitzhüttl *et al*. (2014) and Maniatis *et al*. (2014) carried out experimental investigations on fully tempered thin glass plates with dimensions of $1100 \times 360 \times 2$ mm^2. The maximum vertical displacement attained was 75 mm, corresponding to a strength/stress of around 125 MPa. The vertical displacement *vs*. axial stress curves obtained for different specimens were not consistent and, more importantly, it was not possible to determine an estimate for the tensile strength. Finally, these experiments were complemented with numerical studies to provide further insights on the stress distribution and to assess the influence of the plate thickness, the Young's modulus, and the Poisson's ratio.

The literature review summarized above shows that a standard for testing the strength of thin glass is required in order to enable the structural use of thin glass in civil engineering applications. Hence, new methods of testing must be designed and thoroughly validated to deliver a valid solution that provides consistent and comprehensive results through a standardisable methodology.

In this context, this paper presents experimental and numerical investigations developed with two main goals: (i) to design or adapt existing test setups in order to efficiently determine the strength of thin glass and, if necessary, to propose a new standard test to be used in structural design, and (ii) to characterize thin glass by using those different tests, focusing on the ultimate strength and on the particular behavioural aspect each test reveals more clearly.

For this purpose, a set of analyses and tests were planned in the experimental programme (described in detail in Santos, 2017) comprising the in-plane four-point bending test and the buckling test. Based on the results obtained, a new test method was designed and assessed based on numerical simulations.

2. Material

The material used in the experimental program is an aluminosilicate chemically tempered glass with compressive stresses in the range of 600 MPa to 800 MPa. The samples used were plates with nominal thickness of 2 mm, height of 80 mm and length of 710 mm, with pencil grind edges (C-grind). For the analyses carried out, the relevant properties are as follows: Young's modulus, E = 74 GPa; shear modulus, G = 30 GPa and Poisson's ratio ν = 0.233.

3. In-plane four-point bending test

The main goal of the in-plane four-point bending test is to investigate the ultimate strength of a thin glass sample, taking into account that the most tensioned part of the section is the edge. Similar bending tests to determine the edge strength of regular glass thicknesses have also been performed in other studies, e.g. (Vandebroek 2014). However, in the current study the in-plane loaded thin glass section is much more sensitive to lateral-torsional buckling. Therefore, to determine the ultimate strength of glass, it is of interest to prevent such instability phenomenon.

The advantages of this test method are the following: the four-point bending setup has been thoroughly studied for many applications; it focuses strictly on the edge over a significant length and is the most reliable setup to study the strength of such component; furthermore, if well designed, the behaviour of the sample is linear, not requiring much instrumentation to obtain the intendend results. The main difficulties lie on guaranteeing an effective lateral constraint and on the concentration of stresses on the load application points, where the glass member contacts the metallic parts of the setup.

3.1. Experimental investigations

The basic test setup used in this study is the four-point bending configuration, with 600 mm between supports and 200 mm between loads (Fig. 1). Tests were conducted at a stress rate of 2.0 ± 0.4 MPa/s, following the EN ISO 1288 specifications.

As a complementary material, samples of aluminium of the same dimensions of the thin glass plates were employed (labeled as AL1 to AL7), making use of a material with similar Young's modulus of glass. This aimed at doing preliminary assessment of the test setup using a less expensive material (yet similar), thus preventing compromising thin glass samples.

The lateral constraint used in this test is composed of two 15 mm thick aluminium plates and their final dimensions (after different adjustments) were 710 mm by 80 mm, just like the glass plate (Fig. 2). Between these plates and the test specimen, stripes of Teflon are glued to reduce the friction and a rubber band is placed at supports and load points.

Three versions of the setup, comprising a gradual increase of the stiffness of the lateral constraint system, were tested, mostly on aluminium samples and on one thin glass sample. The tests are described in detail in Santos (2017). In summary, the main features and modifications of the setups were as follows (see illustration in Fig. 2):

a) Setup A - Continuous lateral constraint, leaving some free height at the bottom and top of the glass specimen; outer supports only to bear the lateral constrain, with a span of 400 mm – for samples AL1, AL2;
b) Setup B - Increase of the height of the lateral constraint to cover the whole glass surface; introduction of rubber bands between glass and cross-head – for samples AL3, AL4
c) Setup C - Introduction of two very stiff inner supports; different connection of the machine to the cross-head: spherical for samples AL5, AL6 (as with all previous samples), fixed connection for samples AL7, GLASS.
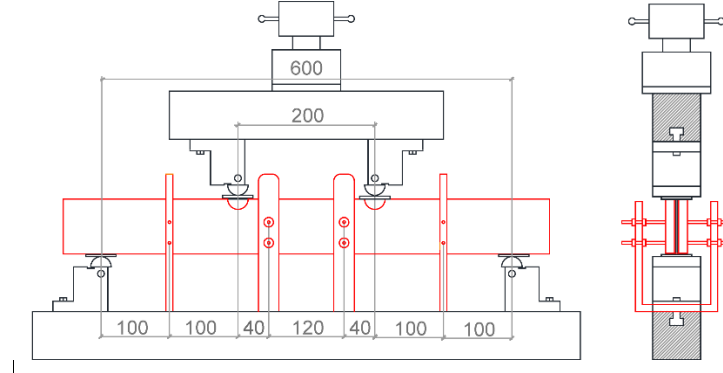

Fig. 1 In-plane four-point bending final setup, front (left) and side (right) views, with focus on dimensions and lateral constraint (red)
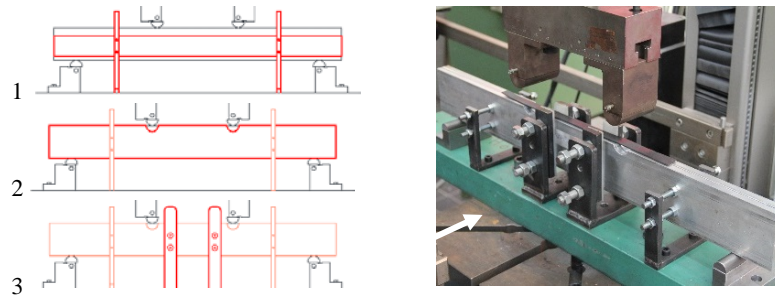

Fig. 2 Iterations of the lateral constraint of the setup and final setup

The results obtained for the final iteration of the test setup are presented in Fig. 3, in terms of load *vs*. cross-head displacement. It is clear that the behaviour is far from linear, which stems from the rubber bands and at some point to instability phenomena. In summary, although the increased stiffness of the lateral constraint allowed reaching much higher values of stress (compared to previous versions of the setup), the mechanical behaviour entails many nonlinearities.
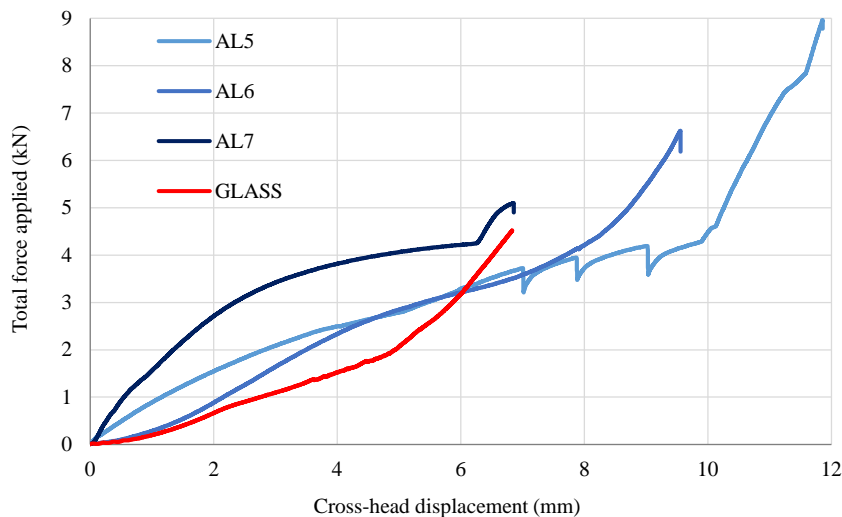

Fig. 3 Force-displacement graph for preliminary tests with aluminium and glass samples, setup C

Besides the nonlinear behaviour, the failure of the glass sample seems to have been caused by a flaw on the edge of the glass (Fig. 4), so no clear conclusions could be drawn regarding strength. A final version of the setup was proposed; however, it was decided to use the remaining samples of thin glass in the buckling tests.

Fig. 4 Detail of a flaw on the edge of the sample tested and corresponding cracking pattern

3.2. Numerical investigations

Numerical investigations (described in detail in Santos, 2017) were conducted about the four-point bending test with two objectives: (i) to study the behaviour of samples without lateral instability and strictly under bending, and (ii) to investigate the lateral-torsional buckling behaviour of test samples with the different setups. Shell finite element models of the various experimental setups used to test aluminium and glass panes were developed (using software DIANA), which included linear buckling instability; herein only the analyses on glass samples (summarized in Fig. 5) are presented. Further details about the models are provided in Santos (2017).

Name	Analysis 1	Validation	Analysis 2	Analysis 3
Goal	Understand the theoretically perfect behaviour of the test, with no lateral displacement	Validate the new model, its geometry and elements used (with many more dof)	Study the lateral torsional buckling phenomenon and the influence of the lateral supports	Study the lateral torsional buckling phenomenon and the influence of the lateral supports
Setup	Perfectly constrained	Setups A and B	Setups A and B	Setup C
dof	Two: $\{u_x, u_y\}$	Five: $\{u_x, u_y, u_z, \phi_x, \phi_y\}$	Five: $\{u_x, u_y, u_z, \phi_x, \phi_y\}$	Five: $\{u_x, u_y, u_z, \phi_x, \phi_y\}$
Lateral constr.	Perfectly constrained	Only outer supports	Only outer supports	Outer and inner sup.
Lateral force	No lateral / horizontal force applied	No lateral / horizontal force applied	Horiz. forces applied proportionally to verti. displacement at loads	Horiz. forces applied proportionally to verti. displacement at loads

Fig. 5 Overview of the set of analyses comprised in the numerical study regarding goals and lateral boundary conditions

Fig. 6 and Fig. 7 illustrate some of the results obtained, namely the stress distributions (at 12 mm of vertical displacement) for analyses 1, 2 and 3. The linear analysis confirmed that the maximum principal stress is mostly located on the edge and this stress distribution is identical to all samples prior to buckling. Concerning the lateral instability analyses, it was shown that the setup is prone to buckling and once it occurs, the stress distribution varies widely along the surface of the glass, preventing the precise assessment of the ultimate strength of glass even in the last iteration. To sum up, even with all improvements, buckling still governs the failure of the thin glass plates.

Analysis 1 — Max (red) = +1024 MPa

Analysis 2 —
Side A: Max (red) = +533 MPa
Side B Max (red) = +377 MPa

Analysis 3 —
Side A: Max (red) = +1371 MPa
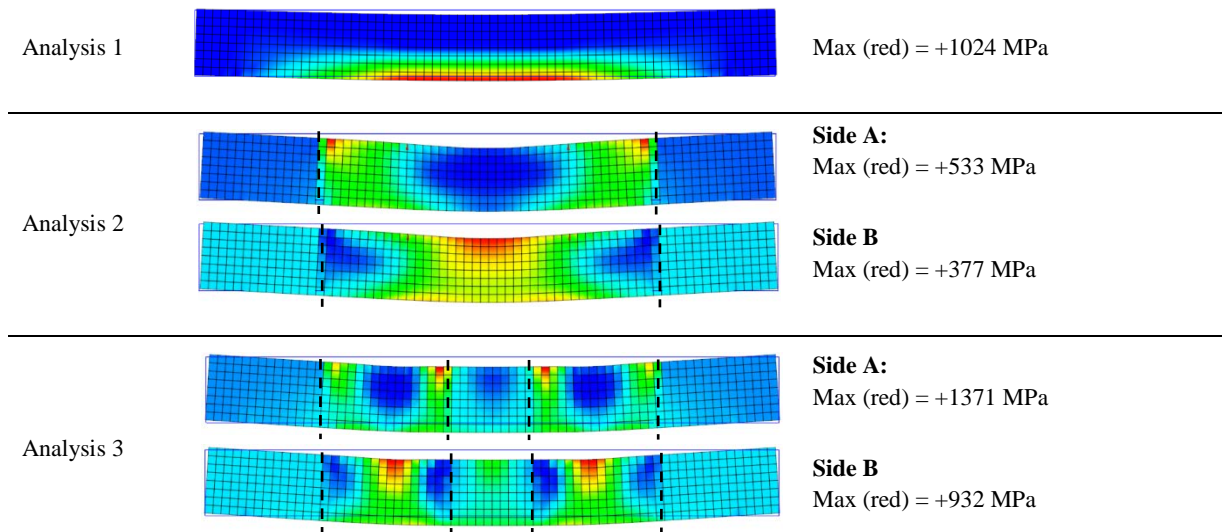**Side B** Max (red) = +932 MPa

Fig. 6 Stress distribution at 12 mm of vertical displacement, for analyses 1, 2 and 3 (lateral supports are indicated with dashed lines)
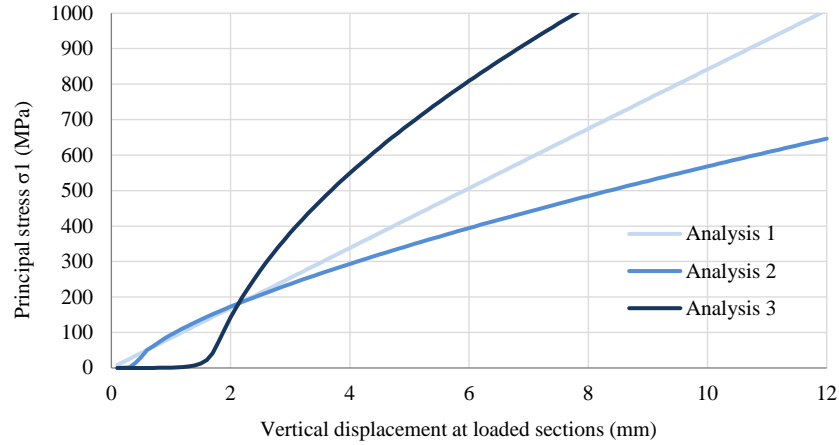
Fig. 7 Principal stress at critical points *vs.* vertical displacement at loaded sections for all three analyses

4. Buckling test

The high potential of application of curved or flexible glass plates of large dimensions motivates the interest in studying their buckling behaviour, besides the assessment of the ultimate strength of the material.

One of the advantages of this buckling test is the introduction of the maximum stress over a considerable area, in a way that is very similar to realistic applications. It allows assessing the performance of thin glass plates in terms of flexibility and curvature.

4.1. Experimental investigations

For the tests conducted herein, the same stress rate of 2.0 ± 0.4 MPa/s set in the EN ISO 1288 specifications was applied.

The buckling test setup, illustrated in Fig. 8, consisted of a glass plate supported at the top and bottom edges by a cylindrical roller that constrained rotations about all axes but the weakest axis of inertia of the plate. The rollers used in the setup have 25 mm of radius and contain a 7 mm deep slit, which could not be deeper due to technical reasons. It is important to mention that the slit has 2.5 mm of width, so it allowed for some movements of the glass plate; a preliminary test with a 2.0 mm wide slit made it very difficult to remove the shatters of the glass specimen after breakage and was thus altered.

The test itself consisted of applying a vertical displacement on the top roller at a rate of 2.085 mm/s (causing an intended axial stress rate of 2,0 MPa/s). In the first stage of the test, a much higher stress rate occurred, but from an axial stress of 200 MPa up to the failure of the samples the planned stress rate was kept roughly constant (Santos, 2017). When a sufficient vertical load was applied, a horizontal displacement was manually and momentarily imposed to set the direction of buckling towards the intended side (protected by an acrylic box).

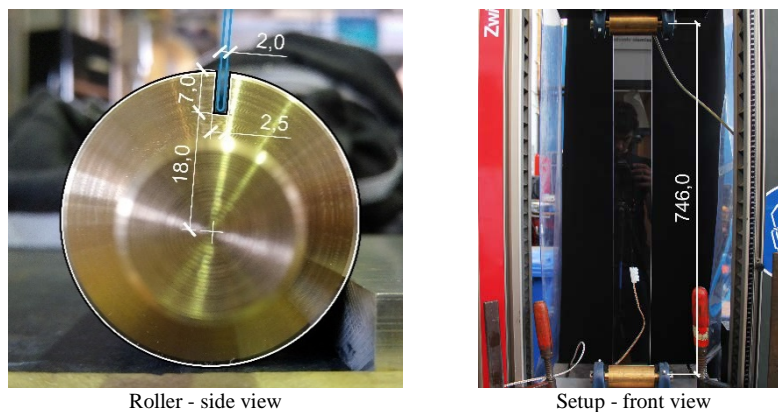Roller - side view   Setup - front view
Fig. 8 Pictures of the test setup with dimensions (mm)

To measure the axial strains, the vertical relative displacement (between rollers) and the corresponding vertical force, the instrumentation consisted of strain gauges, the displacement transducer and the load cell of test machine (*Zwick 010*), as well as videocameras.

The most relevant test results are presented in the subsection 5.3, together with results of numerical simulations.

4.2. Numerical investigations

A numerical analysis was also performed using software DIANA with the main goal of simulating the experimental tests presented above and to obtain a better understanding of the behaviour of the tested plates.

Fig. 9 illustrates the model of the glass plate. Curved shell quadrilateral finite elements with 10 mm of width were chosen and the basic geometry set was a continuous element of $746 \times 80 \times 2$ mm^3. In terms of loads, an initial (horizontal) deformation (1 mm) was introduced by applying a point load in the z-direction at the centre of the plate, thus inducing the consequent buckling, which was then caused by an in-plane displacement (in the x-direction) applied at the top end. The boundary conditions are also illustrated in Fig. 9.

A detailed description of both the preliminary tests and of the instrumentation, as well as of the numerical model (including the loading process, the finite elements used and a study of the initial imperfection) is presented in Santos (2017).
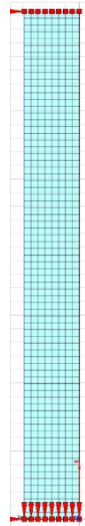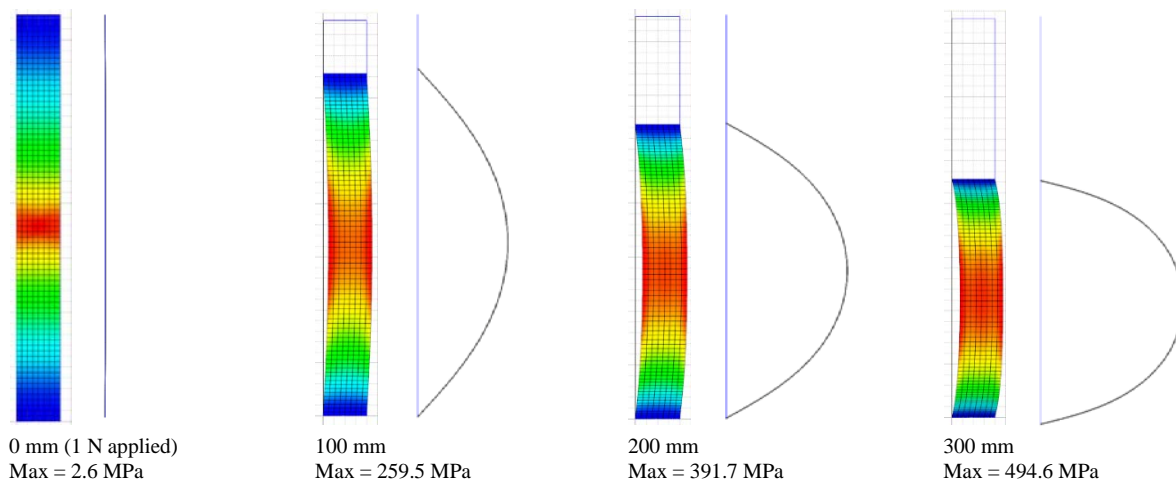
Fig. 9 Geometry, mesh and boundary conditions for the buckling model

4.3. Results

In the following paragraphs, the results of the experimental tests on 10 samples and of the numerical analysis are compared and discussed. This discussion of results starts with the analysis on the applied force, followed by the analysis of stress distributions, concerning both vertical and horizontal stress profiles. Finally, the fracture and strength of thin glass is analysed.

Fig. 10 illustrates the deformation with a side view, produced with the post-processor "midas FX+ for DIANA" with the "actual deformation" option. A qualitative view of the principal stresses σ_1 is also added to each position to complement the graphs presented later; in Fig. 10, the blue represents no tension and red the maximum tension, which is presented below for each case.

0 mm (1 N applied)
Max = 2.6 MPa

100 mm
Max = 259.5 MPa

200 mm
Max = 391.7 MPa

300 mm
Max = 494.6 MPa

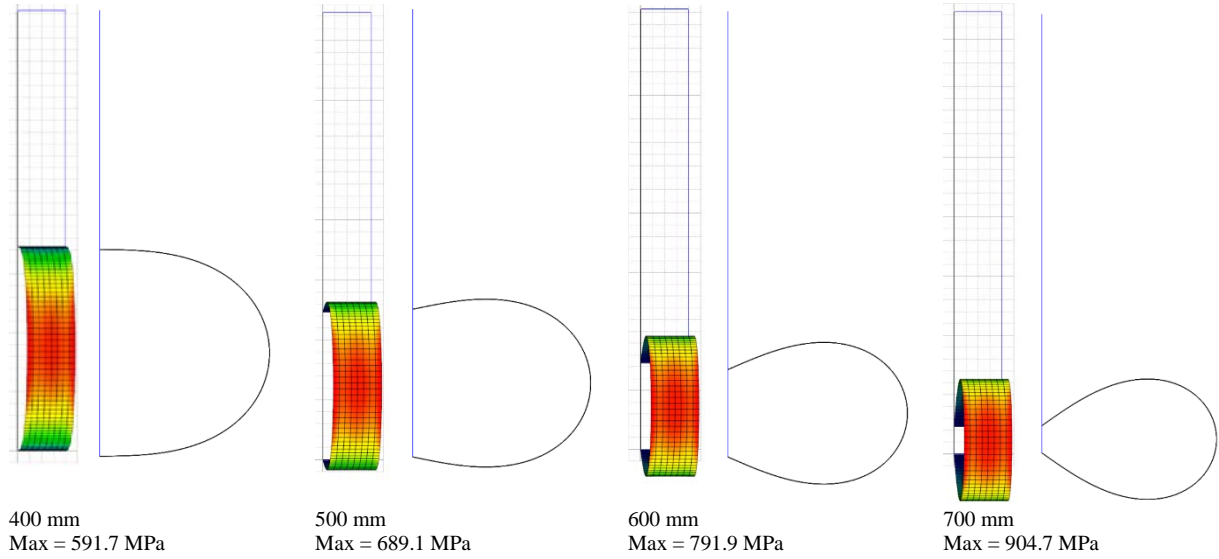| 400 mm | 500 mm | 600 mm | 700 mm |
| Max = 591.7 MPa | Max = 689.1 MPa | Max = 791.9 MPa | Max = 904.7 MPa |

Fig. 11 Side view of the plate deformation and 3D view of principal stress σ_1 along its vertical deformation

Concerning the applied force, the experimental data was obtained with the compression machine and showed remarkable consistency (Fig. 11). The numerical results present slight differences compared to experimental data, particularly regarding the triggering of instability. For both experimental and numerical data, buckling starts at around the same applied force, but while experimental results reveal an increase of force and then a sudden drop with the buckling (which can be due to friction effects), the numerical results initially present a lower force with a much smoother increase of deformation. Then, the behaviour stabilizes and the curves become almost parallel, with an offset of around 5.5 N to 6.5 N. It is worth mentioning that the overall behaviour reflected by the experimental and numerical curves is consistent with the (expected) stable buckling behaviour of an elastic material.
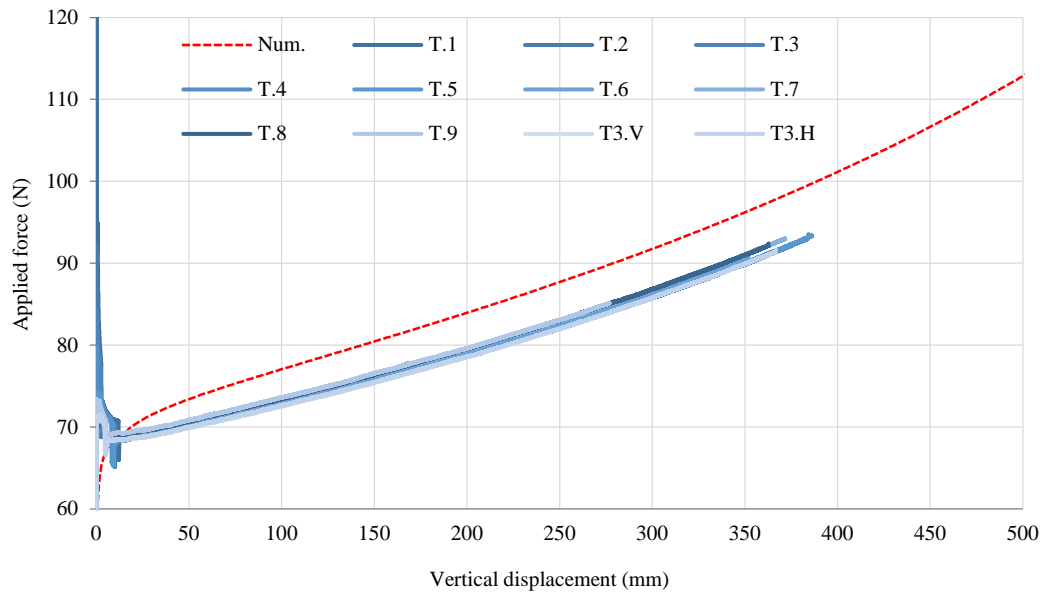

Fig. 11 Applied force vs. vertical displacement, comparison of experimental (T) and numerical (Num) results.

In terms of axial stresses, strains were experimentally measured with a strain gauge at the centre of the glass plates, and then converted to stress by applying the Hooke's Law, considering E=74.0 GPa. As presented in Fig. 12, the numerical behaviour was similar to the experimental data. The results obtained show also that the ratio between numerical and experimental stresses is around 1.35 for lower load levels and then progressively tends to around 1.17.
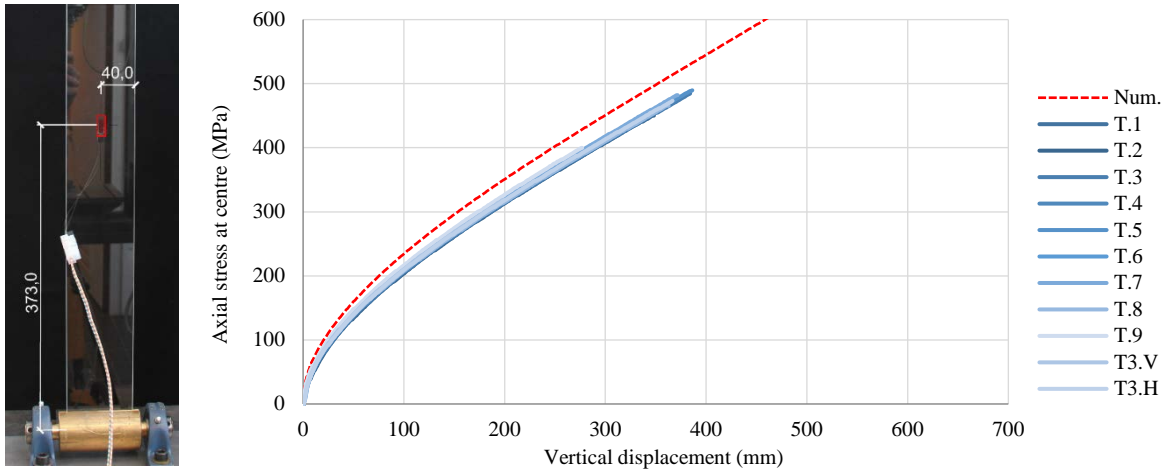
Fig. 12 Left) Strain gauge positioned in the centre of the glass plate; right) stress at centre of outer surface *vs.* vertical displacement, experimental (T) and numerical (Num) results

To obtain the vertical profile of axial stresses, one of the thin glass samples (T3.V) was instrumented with three strain gauges: one at the centre (A) (as all the others presented in Fig. 14) and the two other below the central one at distances of 100 mm (B) and 200 mm (C). For each type of analysis, experimental and numerical, Fig. 15 illustrates the stress ratio between the stress at the centre (A) and at the remaining locations (accordingly, the stress ratio for location A is always 1.00).
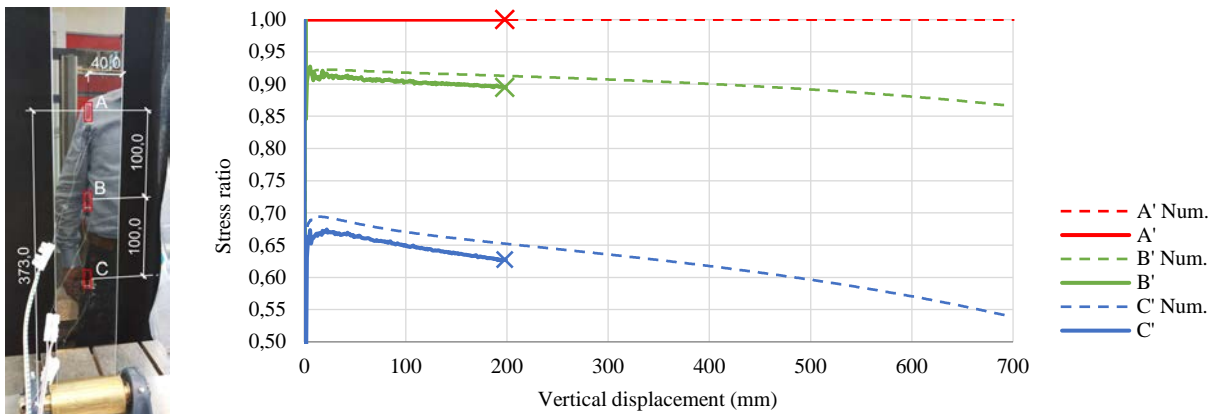

Fig. 13 Left) Three strain gauges displayed along the length of sample T3.V; right) Numerical and experimental vertical distribution of axial stress vs. vertical displacement; comparison and ratio

Fig. 14 presents the results of a similar analysis, which now focused on the horizontal profile of axial stresses. With that purpose, one of the thin glass samples was instrumented with three strain gauges at mid-height: two near the edge of the plate, but still in the plane surface (A and C), and one at the centre (A), as all the others presented in Fig. 12. The overall behaviour of experimental and numerical curves is also quite similar, revealing that the stresses at the edges are 1.18 to 1.09 times higher than at the centre. For the width of the section, the experimental to numerical ratio is almost identical.
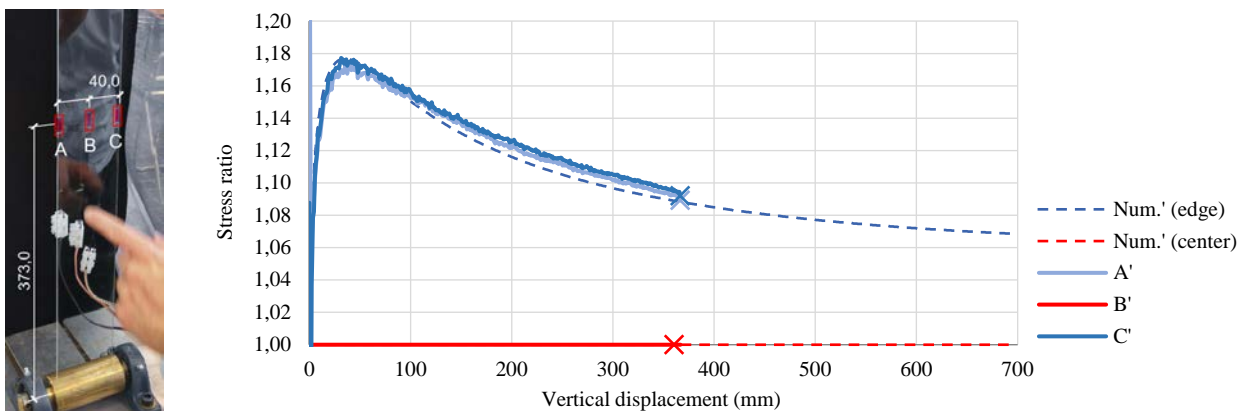

Fig. 14 Left) Three strain gauges displayed along the width of sample T3.H; right) numerical and experimental horizontal distribution of axial stress vs. vertical displacement; comparison and ratio

In spite of the above-mentioned success in terms of coherency and consistency of experimental results, the plate was not fully clamped in the rollers' slits. In fact, this factor had some influence in the experimental behaviour, which justifies the differences to the numerical results. The illustration depicted in Fig. 16 clarifies this problem: with the setup used the glass-metal contact is located on very thin lines and the centre of the roller is not perfectly aligned with the axis of the plate. To sum up, the glass to metal contact at the slit, not considered in the numerical analysis, affects the results obtained from the tests, namely the actual length of the glass plate, as well as the local stress distribution.

Moreover, and more importantly, the ultimate strength/collapse seems to have been caused precisely by the contact of the glass plate with the rollers, as attested by video frames (Fig. 15) and by a geometrical analysis of the supports area. The glass/metal contact is located on very thin lines and there is not any auxiliary material to distribute the local stresses that are developed, so the maximum stress attained is likely limited by the setup.

Fig. 15 Frames of the collapse, highlighting the frame the glass breaks at the slits (centre picture) and the following frame (right picture)

Fig. 16 also illustrates a proposed alternative setup, including a deeper slit and a neoprene band, which provides the following potential advantages: (i) the lower elastic modulus of neoprene provides a much better (more uniform) local stress distribution in the slit; (ii) the applied loads are rather low, so the resulting stresses and deformations at the neoprene will be negligible; (iii) the behaviour is close to clamped and allows more easily removing the glass shatters after the collapse; (iv) the centre of the roller is coincident with the end of the glass plate, making the height of the setup the same as the height of the plate; (v) finally, it allows increasing the range of glass thicknesses possible to test, simply by combining the glass thickness with an appropriate thickness of the neoprene band. To conclude, the proposed geometry seems to offer many benefits over the former setup, mainly leading to a design compliant with standard sizes and providing a much closer agreement with the theoretical behaviour expected for well-defined boundary conditions; it is an upgraded version of the one that was used in the tests and could stand as a standard test.
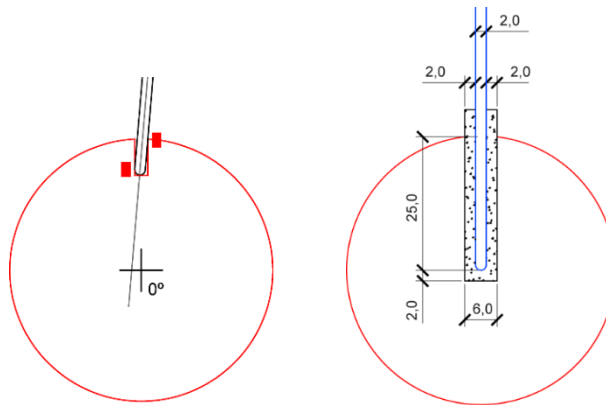

Fig. 16 Contact areas (red) between glass and metallic roller and proposed setup

The stresses obtained were in the range of 300 to 400 MPa. Once more, note that the stresses obtained from these analyses are a lower bound of the actual tensile strength of the thin glass tested, as failure was prematurely caused by the stress concentrations at the slits of the cylinders.

5. Brief discussion about the tests performed

The two test setups developed and presented in the previous sections provided interesting insights on the behaviour of thin glass and on the procedures to test it. However, both tests presented problems regarding their application or standardization.

The four-point bending test is a rather complex test to perform correctly due to the high forces at stake and the very thin section that quickly becomes unstable, even with lateral constraints.

The buckling test was fairly easy to set as the geometrical nonlinearities are easily predictable and are even used as part of the test principle, leading to very consistent test results. However, the test principle is closely related to the minimum curvature radius of the glass plate, which depends on its thickness and on the ultimate strength of glass. Hence, very thin plates or the ever growing strength of glass pose considerable difficulties to the experimental determination of the ultimate strength of glass and might compromise the applicability of this type of test.

Therefore, an alternative testing method, the tension test, was designed. The goal of this test, presented in the next subsection, is to be able to be applied to any thickness and strength, and become the standard for the testing of thin glass. Due to time restrictions, it was not yet possible to assess this test; therefore, only results of numerical analysis are presented.

6. Proposal of a new test to study the strength of thin glass: tension test

The main goal of the tension test is to study the behaviour of glass under pure tension and to determine its ultimate strength. The test proposed herein has the advantage of subjecting almost the entire length of the glass plate to the maximum stress, with the particularity of not being prone to any kind of instability or nonlinearity. Therefore, it can be applied to any thickness, providing a measurement of the ultimate tensile strength.

The difficulties of the test proposed lie in the geometry of the specimen: a uniform rectangular plate with constant cross section along the whole length. Usually, specimens used for tensile tests have a dog-bone shape (with a thicker and/or wider part); with such geometry, although stress concentrations develop in the load transfer, failure does not occur at the critical section. However, that type of section is not possible to implement in (thin) glass samples; directly gripping glass plates is also not possible. Therefore, a glued connection is proposed for the test presented here.

The setup consists of two pairs of metallic plates (with geometry of $150 \times 100 \times 10$ mm^3) that are glued with a proper adhesive, in an overlap length of 60 mm, to both sides of the glass plate (with geometry of $710 \times 80 \times 2$ mm^3). The metallic plates - a pair for each extremity of the glass plate - assure the connection of the glass specimen to the tensile machine; this connection is done through a steel cylinder inserted in a hole of the same radius in the metallic plates (Fig. 17).
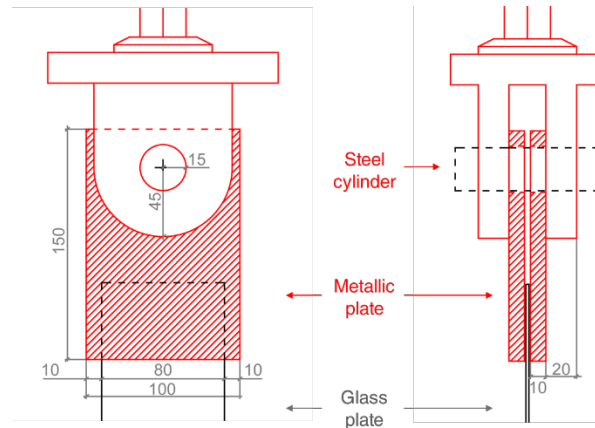

Fig. 17 Tension test setup, front (left) and side (right) views

The numerical analysis presented next had the main goal of predicting the behaviour of the glued connection and the distribution of stresses in the different materials. The finite element models of the test setup (described in detail in Santos, 2017) were developed using software DIANA.

The glass was modelled as a linear material with elastic and shear moduli of 74 GPa and 30 GPa, respectively. A commercially available glue (*Ultra Light-Weld® 431* by DYMAX) was selected and deemed as appropriate, being modelled as a nonlinear elasto-plastic material with a von Mises yield stress of 23 MPa and an elastic modulus of 574 MPa. Neither the Poisson's ratio nor the shear modulus were provided by the manufacturer, but the study by Nhamoinesu & Overend (2012) on similar glass-steel adhesives reported a range of values for the Poisson's ratio (ν) from 0.29 to 0.48. Therefore, these two Poisson's ratios were used to study its impact on the behaviour of the test and cover the whole range expected for this material property. Herein, more focus is given to the lowest value, as it was found to provide better results.

From the analysis of the applied force *vs.* the displacement at the outer surface of the adhesive, illustrated in Fig. 18, it is evident that the Poisson's ratio is not relevant for the applied force. Six points covering the linear and yielding phases of the adhesive are highlighted and used later in this section to illustrate the analyses of the stress distribution.
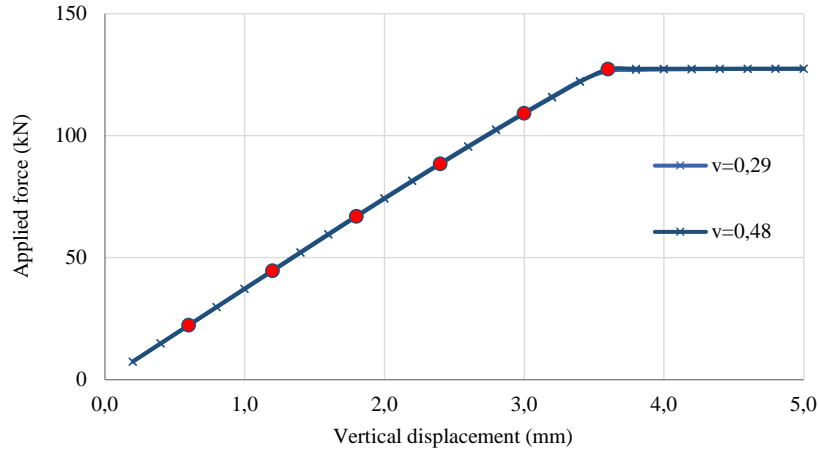
Fig. 18 Numerical results of applied force *vs.* vertical displacement at the outer surface of the adhesive

The analysis of the stresses developed at the glass surface was carried out by plotting the values of the principal stress σ_1 on the centre (C) and on the edge (E) for the six force-displacement points presented in Fig. 18 over a profile of 80 mm starting from the top of the glass plate and for $\nu = 0{,}29$ (Fig. 19). The stresses reach 800 MPa and are quite homogeneous, without relevant peaks. This is due to the relatively low stiffness of the adhesive, providing a smooth/uniform load transfer between the glass and steel plates. The glass plate is expected to fail, thereby providing strength results; otherwise, a larger adhesive area is required.

A similar analysis was carried out about the surface shear stress profile over the bonded length (60 mm). For the referred six load values listed, the shear stresses at the centre and at the edge along the bond length were computed for $\nu = 0.29$ (Fig. 20). The yielding of the adhesive occurred for stresses of 13.3 MPa, which is in agreement with the von Mises yield stress set as input.
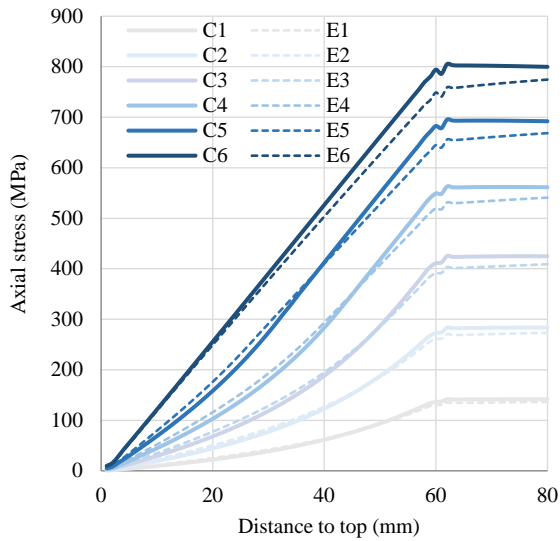

Fig. 19 Evolution of centre (C) and edge (E) axial stresses in the glass plate, vertical profile ($\nu = 0.29$)
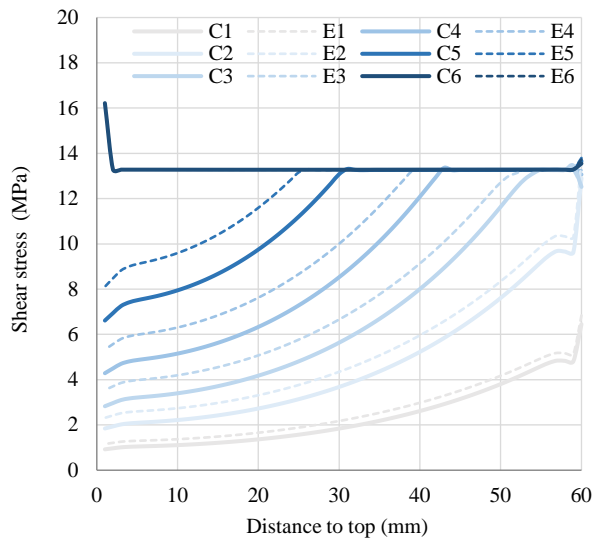
Fig. 20 Evolution of centre (C) and edge (E) shear stresses in the adhesive, vertical profile ($\nu = 0.29$)

7. Conclusions

The main conclusions obtained in this study were derived from both the material characterization and destructive tests and are as follows.

The **four-point in-plane bending test** required a significant development of the conventional setup, including several iterations to overcome the various difficulties that were encountered. Together with the numerical analyses, it is concluded that if thin glass is subjected to in-plane loading, lateral instability is a serious concern and it is not easy to effectively prevent this phenomenon. Furthermore, such instability significantly affects the stress distribution in the bring of collapse, rendering it impossible to determine the strength of thin glass.

The principle of the **buckling test** is based on the geometrically nonlinear deformations developed in the specimen. With the setup used, as expected, it was possible to cause very significant deformations in the test specimens. The test provided very coherent and consistent experimental results in terms of applied forces and stresses (strains), whose behaviour was well simulated in the numerical analysis. However, the tests were affected by the slit of the roller, which not only justifies the slight differences between

experimental and numerical data, but also seems to have caused the premature collapse of the specimens, due to the stress concentrations at the slits. Therefore, the maximum stress values attained, in the range of 300 to 400 MPa, are a lower bound of the strength of thin glass.

In this context, an alternative test was finally proposed, the **tension test**, which seems to be the one with the most potential in terms of application and standardization, provided that the issues concerned with the adhesive connection are dealt with correctly. The numerical study revealed that the nonlinearity and elongation of the adhesive suggested to be used to bond the glass plate to the metallic plates provides a very homogeneous load transfer from the glass being tested to the outer surface of the metallic plates of the test fixture. The main advantages of this test over the former two are the following: (i) the thickness or strength of the thin glass samples are less likely to compromise the collapse of the test specimen (as the curvature radius is not involved); (ii) the portion of the glass area subjected to the maximum stress compared with the total area is much higher; (iii) the test is dominated by a geometrically linear behaviour; and (iv) the yielding of the adhesive allows for a quite homogeneous load transfer, and although it introduces some nonlinearity in the force-displacement response, the stress develops linearly in most of the glass area. Further experimental investigations are needed to validate the test procedure proposed herein.

Acknowledgements

References

Aben, H., Anton, J., & Errapart, A. (2008). Modern Photo elasticity for Residual Stress. (B. P. Ltd, Ed.) Strain 44, 40-48.

Aben, H., Anton, J., Errapart, A., Hödemann, S., Kikas, J., Klaassen, H., & Lamp, M. (2010). On non-destructive residual stress measurement in glass panels. Estonian Journal of Engineering, 16, 150-156.

AGC. (2014). Technical Specifications – Leoflex^(TM) . AGC.

Albus, J., & Robanus, S. (2015). Glass in Architecture - Future developments. Detail.

Corning. (2016). Corning - How it's Made. Retrieved from Corning: http://www.corning.com/

Corning. (2017). Corning – Product Sheet Corning® Gorilla® Glass 5. Retrieved from Corning: http://www.corning.com/

EN 1288:2000 Glass in building - Determination of the bending strength of glass. Brussels: European Committee for Standardization (CEN).

GlasStress Ltd. (2013). SCALP Instruction Manual Ver. 5.8.2. GlasStress Ltd.

Holzinger, P. (2011). Thin glass technology for insulating glass production. Glass Performance Days. Finland: GPD.

Jiang, L., Guo, X., Li, X., Li, L., Zhang, G., & Yan, Y. (2012). Different K+–Na+ inter-diffusion kinetics between the air side and tin side of an ion-exchanged float aluminosilicate glass. Applied Surface Science, 265, 889-894.

Maniatis, I., Nehring, G., & Siebert, G. (2014). Studies on determining the bending strength of thin glass. ICE Publishing. Structures and Buildings, 169, 393-402.

Neugebauer, J. (2015). A Movable Canopy. International Conference on Building Envelope Design and Technology. Graz.

Neugebauer, J. (2016a). Determining of Bending Tensile Strenght of Thin Glass. Challenging Glass 5. Ghent.

Neugebauer, J. (2016b) What is Thin Glass? GlassCon Global Conference Proceedings, Boston, 2016

Nhamoinesu, S., & Overend, M. (2012). The Mechanical Performance of Adhesives for a Steel-Glass Composite Façade System. Challenging Glass 3. TU Delft: Challenging Glass 3.

Santos, F. O. (2017). Testing the strength of thin glass. Master dissertation in Civil Engineering. Lisbon: Instituto Superior Técnico, University of Lisbon.

SCHOTT. (2014 a). Technical Glasses - Physical and Technical Properties. SCHOTT.

SCHOTT. (2014 b). Product datasheet – SCHOTT Xensation® Cover. SCHOTT.

Schneider, J. (2015). Thin Glasses - A future envelope? Conference on Building Envelopes. Delft: TU Delft.

Siebert, G. (2013). Thin glass elements - a challenge for new applications. Glass Performance Days 2013, (pp. 316-319). Tampere, Finland.

Spitzhüttl, J., Nehring, G., & Maniatis, I. (2014). Investigations on determining the bending strength of thin glass. Challenging Glass 4 & COST Action TU0905 Final Conference (pp. 521-530). Leiden: CRC Press/Balkema.

Vandebroek, M. (2014). Thermal Fracture of Glass. Gent & Antwerpen: Universiteit Gent & Universiteit Antwerpen. PhD thesis in Civil Engineering.